Vol. 3 No. 1 Edisi Januari 2026 E. ISSN. 3032-2472
Multidisciplinary Indonesian Center Journal (MICJO)
Journal page is available to
https://e-jurnal.jurnalcenter.com/index.php/micjo
Email: admin@jurnalcenter.com

STUDY OF PHOTOCATALYTIC HYDROGEN PRODUCTION OVER Ni-DOPED ZnO AND TiO_2 PHOTOCATALYSTS VIA CHEMICAL STABILIZATION

STUDI PRODUKSI HIDROGEN FOTOKATALITIK PADA FOTOKATALIS Ni-DOPED ZnO DAN TiO_2 MELALUI STABILISASI KIMIA

Frendi Maulana[1*], Yohanes Engge[2]

[1*]Universitas Nahdlatul Ulama Lampung, Email: frendimaulana270@gmail.com
[2]Universitas Nahdlatul Ulama Lampung, Email: engge_yohanes@yahoo.com

*email koresponden: frendimaulana270@gmail.com

DOI: https://doi.org/10.62567/micjo.v3i1.2314

Abstract

This study synthesized Ni-doped ZnO (Ni0.05Zn0.95O) and TiO2 (Ni0.05Ti0.95O2) via immersion-assisted coprecipitation for hydrogen production. UV-Vis confirmed bandgap reduction to 2.87 eV (ZnO) and 2.82 eV (TiO2), enabling visible light activity. XRD and SEM verified Ni incorporation and a significant reduction in crystal size (to 21 nm). To mitigate rapid particle sedimentation (25 min), sodium silicate was applied as a dispersant, successfully extending suspension stability to 4 hours. Notably, this chemical stabilization maintained a lower reactor temperature (49°C) compared to mechanical stirring (52°C), preventing efficiency loss due to thermal effects. Ni0.05Zn0.95O exhibited the highest photocatalytic activity, attributed to its superior Ni atomic composition. This research demonstrates that combining Ni-doping with chemical dispersion effectively optimizes both the electronic and physical properties of photocatalysts for enhanced hydrogen harvesting.

Keywords : photocatalysis, hydrogen production, nickel doped, TiO2, ZnO.

Abstrak

Penelitian ini menyintesis fotokatalis ZnO terdoping Ni (Ni0.05Zn0.95O) dan TiO2 (Ni0.05Ti0.95O2) melalui metode ko-presipitasi berbantuan perendaman (immersion-assisted co-precipitation) untuk produksi hidrogen. Analisis UV-Vis mengonfirmasi penurunan celah pita (bandgap) menjadi 2,87 eV (ZnO) dan 2,82 eV (TiO2), yang memungkinkan aktivitas di bawah cahaya tampak. XRD dan SEM memverifikasi inkorporasi Ni dan pengurangan signifikan pada ukuran kristal (hingga 21 nm). Untuk memitigasi sedimentasi partikel yang cepat (25 menit), natrium silikat diaplikasikan sebagai agen pendispersi, yang berhasil memperpanjang stabilitas suspensi hingga 4 jam. Secara khusus, stabilisasi kimia ini menjaga suhu reaktor tetap rendah (49°C) dibandingkan pengadukan mekanis (52°C), sehingga mencegah penurunan efisiensi akibat efek termal. Sampel Ni0.05Zn0.95O menunjukkan aktivitas fotokatalitik tertinggi, yang disebabkan oleh komposisi atomik Ni yang lebih unggul.

Multidisciplinary Indonesian Center Journal (MICJO)
Journal page is available to
https://e-jurnal.jurnalcenter.com/index.php/micjo
Email: admin@jurnalcenter.com

Penelitian ini membuktikan kombinasi doping Ni dengan dispersi kimia efektif mengoptimalkan sifat elektronik dan fisik fotokatalis untuk meningkatkan produksi hidrogen.

Kata Kunci : fotokatalisis, produksi hidrogen, doping nikel, TiO2, ZnO.

1. INTRODUCTION

The photocatalytic process is initiated when photon activates the semiconductor. The absorbed photon energy must create a lone pair of electrons with an energy of at least 1.23 eV and at most 3.0 eV for the visible light range. The looking for visible light-responsive semiconductors must be undertaken considering that the solar spectrum is dominated by ultraviolet (5%), visible light (43%), and infrared (52%). Ideal semiconductors must also have requirements of low fabrication costs, non-toxicity, chemical stability, corrosion resistance, and an appropriate bandgap. Photocatalysts that are widely used include, for example WO3, Fe_2O_3, $FeTiO_3$, SnO_2, $MnTiO_3$, CdS, PbS, TiO_2, and ZnO (Engge et al., 2021; Gupta & Tripathi, 2011; Istiroyah et al., 2021). For photocatalytic water separation, external energy is often required to trigger the process. Fe_2O_3 exhibits a short-lived charge transfer and signs of photo corrosion than TiO_2 and ZnO. Meanwhile, it is believed that binary metal sulfide semiconductors such as CdS, CdSe, GaAs, and PbS are not stable enough as catalysts in aqueous media because they are prone to photo corrosion and toxic (A. Mills and S. Le Hunte, 1997; Beydoun et al., 1999). Therefore, TiO2 and ZnO are considered potential among the photocatalysts for water splitting. However, in a single application, the wide bandgap is sufficient to inhibit the mobility of electron transfer from the valence band to the conduction band. As a result, electron-hole recombination can quickly occur (Mintu Ali et al., 2021) and certainly limits the dissociation performance of water separation. To overcome this limitation, modifying the crystal structure and the material morphology by inserting transition metals such as Ni, Fe, Al, Co, Mn, is necessary. Metal ions doped on the semiconductor surface, such as TiO_2 can change the redox sites of photocatalytic reactions in irradiation response. For example, the metal can act as an electron acceptor under UV irradiation and as an electron injector under visible irradiation (Murakami et al., 2008).

In recent years, Physico-chemical techniques have been used for materials fabrication, including sol-gel (Anna V. Abramovaa,⁎ , Vladimir O. Abramova, Vadim M Bayazitova & Elena A. Straumalb, Sergey A. Lermontovb, Tatiana A. Cherdyntsevac, Patrick Braeutigamd, Maik Weißed, 2020), co-precipitation (Pavithra & Jessie Raj, 2021), sonochemistry (Luévano-Hipólito & Torres-Martínez, 2017), microwave (Mallikarjunaswamy, C Lakshmi Ranganatha, V Ramu et al., 2019), hydrothermal (Shahi et al., 2020), etc. Our study is aimed to develop an immersion-assisted co-precipitation technique to synthesize Ni-doped ZnO and TiO2 materials. Ni is a good conductor of heat and electricity and resists corrosion. It has an electron configuration of [Ar] 3d8 4s2 where, according to Hund's rules, the 3d orbital has two unpaired electrons that assist its binding on the catalyst surface throug coordinate covalent bonds. In addition, nickel is often chosen as a ZnO dopant because the size of the Ni^{2+} ionic radius (0.069 nm) is close to that of the Zn^{2+} (0.074 nm) ion, which has the same valence and structure. The

Multidisciplinary Indonesian Center Journal (MICJO)
Journal page is available to
https://e-jurnal.jurnalcenter.com/index.php/micjo
Email: admin@jurnalcenter.com

substitution effect of Ni^{2+} in the Zn^{2+} lattice provides more charge carriers without changing the hexagonal crystal structure. Ni atoms are useful as dopant donors forming shallow donors below the conduction band, so the conduction band position is lower than the previous position (Elilarassi & Chandrasekaran, 2011; Singh et al., 2015). This causes a decrease in the required activation energy and shifts the absorption edge into the visible range. Specifically, a 5% Ni concentration has been shown to yield a significant reduction in bandgap and transmittance (Gnanamozhi et al., 2020).

In this study, we report the synthesis of Ni-doped ZnO and TiO_2 photocatalysts via an immersion-assisted co-precipitation technique. Beyond electronic modifications, this work addresses the physical challenges of photocatalysis by utilizing sodium silicate as a dispersing agent to mitigate the rapid sedimentation of the nanopowders. Furthermore, we evaluate how this chemical stabilization influences the system's thermal profile, providing a solution to the unwanted temperature increases often encountered in mechanical stirring. The resulting photocatalysts were characterized using XRD, SEM-EDX, and UV-Vis spectroscopy, and their performance was evaluated through hydrogen gas production via photocatalytic water splitting.

2. RESEARCH METHOD

The preparation of the $Ni_{0.05}Zn_{0.95}O$ photocatalyst was started by dissolving 7.7536 g of the precursor $Zn(CH_3CO_2)_2.2H_2O$ which was equal to 0.5406 g $Ni(NO_3)_2.6H_2O$ in 50 mL of distilled water. The solution was vigorously stirred with a magnetic stirrer at room temperature for 1 hour, followed by the addition of 50 mL NaOH 1 M to the solution, and the mixture was stirred for another 1 hour. The solution was then sonicated at 70 °C for 2 hours. After that, the soaking process was continued overnight. The precipitate formed was filtered and washed in an aquadest environment. It is washed to remove the sodium ion content in the precipitate. Finally, the light green precipitate was dried in an oven at 100 °C to dryness. The dry product was then calcined at 500 °C for 2 hours.

The preparation of the $Ni_{0.05}Ti_{0.95}O_2$ photocatalyst starts with the preparation of a solution from a mixture of titanium(IV) isopropoxide $Ti[OCH(CH_3)_2]_4$ and 143 mL C_2H_5OH. Separately, a solution was made from a mixture of 3 mL concentrated HNO_3, 143 mL C_2H_5OH, and 15 mL distilled water. The two solutions were mixed slowly and then stirred vigorously at room temperature for 1 hour. A solution of 2.1565 g $Ni(NO_3)_2.6H_2O$ and 10 mL distilled water was then added beforehand and the resulting mixture was stirred further again for 1 hour. Then, sonication was performed at 70°C for 2 hours. The homogeneous solution was then allowed to stand for 24 hours, during which time a precipitate formed and dried in an oven at 100°C. Finally, the calcination process was carried out at a temperature of 500°C for 2 hours. The photocatalyst $Ni_{0.05}Ti_{0.95}O_2$ and $Ni_{0.05}Zn_{0.95}O$ nanopowders were characterized using UV-Vis, XRD, and SEM-EDX assays. The setup for the photocatalytic hydrogen production reactor was adopted from a previous study (Engge et al., 2023; Maulana et al., 2022, 2024).

Multidisciplinary Indonesian Center Journal (MICJO)
Journal page is available to
https://e-jurnal.jurnalcenter.com/index.php/micjo
Email: admin@jurnalcenter.com

3. RESULT AND DISCCUSSION

a. UV–visible characterization

Figure 1(a) shows the absorption of UV-vis radiation by the photocatalyst material. The spectrum confirmed a higher wavelength absorption shift of the nickel-doped synthesized material. In the wavelength range of visible light (400-800 nm), $Ni_{0.05}Zn_{0.95}O$ material shows two apparent absorption peaks formed around 455 nm (1.55 eV) and 660 nm (0.68 eV). This is due to the crystal field splitting of the $3d^8$ orbitals and charge transfer from $Ni^{2+} \rightarrow Zn^{2+}$. It is believed that the active absorption shift to the visible light region is due to the insertion of Ni^{2+} ions between the ZnO lattice during the sonication process (materials synthesis stage). The longer the sonication is carried out, the stronger the electron exchange interactions in the *sp-d* orbitals. This interaction causes the density of electrons to decrease and the energy gap to fall (Selvinsimpson et al., 2021),(Pavithra & Jessie Raj, 2021). In the end, Ni concentration up to 5% in ZnO could increase the absorption edge from ultraviolet wavelengths to visible wavelengths.

The same applies to $Ni_{0.05}Ti_{0.95}O_2$, which also experience an absorption shift into the visible light range. Two apparent absorption peaks were detected around 440 nm and 750 nm, corresponding to sub-band gaps of 2.37 eV and 0.79 eV, respectively. In another study, such a peak occurs due to a crystal plane splitting, the $3d^8$ band associated with the Ni^{2+} ion split up into form two sub-bands of charge transfer $Ni^{2+} \rightarrow Ti^{4+}$ has been reported (Ganesh et al., 2012; Lin et al., 2006). Finally, a significant shift of the absorption edge towards the visible region supports $Ni_{0.05}Zn_{0.95}O$ and $Ni_{0.05}Ti_{0.95}O_2$ material's effective photocatalytic activity in the future. The absorption coefficient of the material is related to the excitation coefficient, with increasing absorption edge decreasing the energy gap.

Figure 1(b) is a plot of the optical bandgap energy of the photocatalyst determined by the Tauc method. The correlation between the graphs of Figure 1 show that the further shift of the absorption band edge to a higher wavelength causes a decrease in the bandgap energy. The energy band gap narrowed after the material synthesis from 3.20 eV (pure ZnO) to 2.87 eV ($Ni_{0.05}Zn_{0.95}O$) and from 3.28 (pure TiO_2) to 2.82 eV ($Ni_{0.05}Ti_{0.95}O_2$). A similar study reported bandgap reduction after Ni doping using an ultrasonically assisted co-precipitation technique (Gnanamozhi et al., 2020). Here the Ni^{2+} ion is emphasized; it acts as a defect in the valence band to reduce the bandgap energy.

Multidisciplinary Indonesian Center Journal (MICJO)
Journal page is available to
https://e-jurnal.jurnalcenter.com/index.php/micjo
Email: admin@jurnalcenter.com

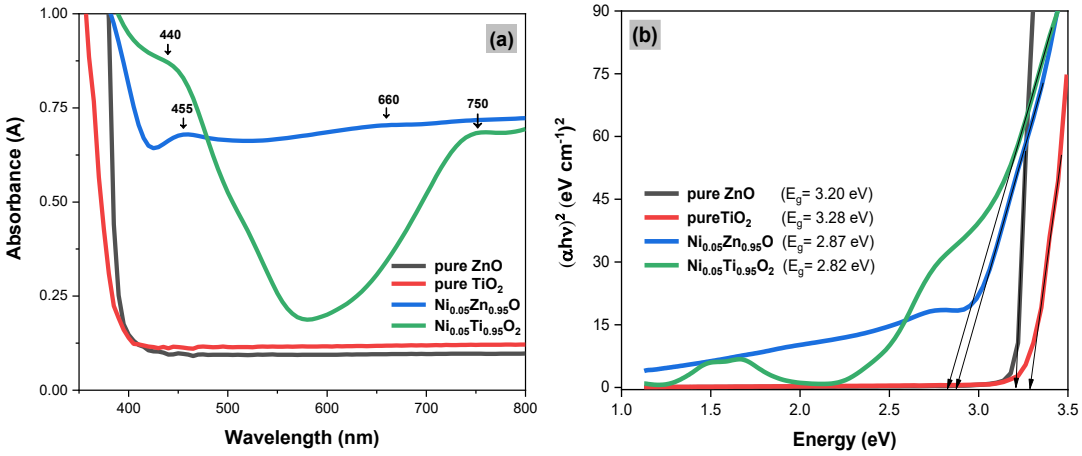

Figure 1 (a) UV-vis absorbance spectrum, (b) Bandgap energy of the photocatalyst material

b. XRD characterization

The diffractogram pattern of $Ni_{0.05}Zn_{0.95}O$ and $Ni_{0.05}Ti_{0.95}O_2$ nanoparticles in the range of 2θ (20º-80º) are shown in Figure 5. The field intensity peaks 25.26º, 36.95º, 37.80º, 38.57º, 48.04º, 54.02º, 55.01º, 62.63º, 68.84º, 70.26º, 75.06º for $Ni_{0.05}Ti_{0.95}O_2$ nanoparticles are all represent the anatase crystal phase of the tetragonal system according to the Crystallography Open Database or COD (entry number 96-900-9087). In addition, another peak is formed at an angle of 27.34º assigned to Ni atom based on COD (entry number 96-153-3685). In addition, the diffraction peak of $Ni_{0.05}Zn_{0.95}O$ nanoparticles was confirmed to show a hexagonal crystal system having a zincite (wurtzite) structure according to COD (entry number 96-900-8878). The orientation of the *hkl* field (Miller index) at angle positions 31.77º, 34.43º, 36.27º, 47.57º, 56.63º, 62.89º, 66.41º, 67.99º, 69.09º, 72.61º, 76.93º, 77.11º are characteristic peaks of ZnO crystals, while the other new peaks corresponds to $Ni_{0.9}OZn_{0.1}$ at 37.21º, 43.23º, 62.89º, 75.25º, 79.19º. One study reported NiO peaks were formed due to the solubility of the dopant exceeding the solubility threshold of ZnO as the host matrix (Singh et al., 2015). Here, NiO phase is very possible to explain as the composition of Ni (0.05), almost near to (0.06) which is shown to have an octahedral coordination system with a radius of Ni^{2+} (83 pm) much larger than the size of the Zn^{2+} ion (74 pm) in the host lattice (Samanta et al., 2018). Based on the Figure 2, the position of diffraction peak decreases with increasing Ni^{2+} ion content at a lower intensity. A decrease in intensity can indicate a reduction in crystallinity and broadening of the diffraction peaks that indicates a reduction in crystal size, as shown in Figure 2 and Table 1. The reason is that appear to the growth of NiO amorphous and the separation of Ni^{2+} atoms as defects at the grain boundaries (Bouaoud et al., 2013). By observing the sharpest peaks of the diffractogram curve, the crystal size was calculated using the Debye-Scherer equation. Interestingly, the average crystal size was achieved on the nanoscale (aggregate smaller than 100 nm). The average crystal size at a 2θ angle is shown in Table 1.

Multidisciplinary Indonesian Center Journal (MICJO)
Journal page is available to
https://e-jurnal.jurnalcenter.com/index.php/micjo
Email: admin@jurnalcenter.com

Table 1. The average particle size calculated using the Debye-Scherer equation

Materials	Average crystal size (nm)
pure ZnO	65.32
$Ni_{0.05}Zn_{0.95}O$	22.47
pure TiO_2	90.46
$Ni_{0.05}Ti_{0.95}O_2$	21.02

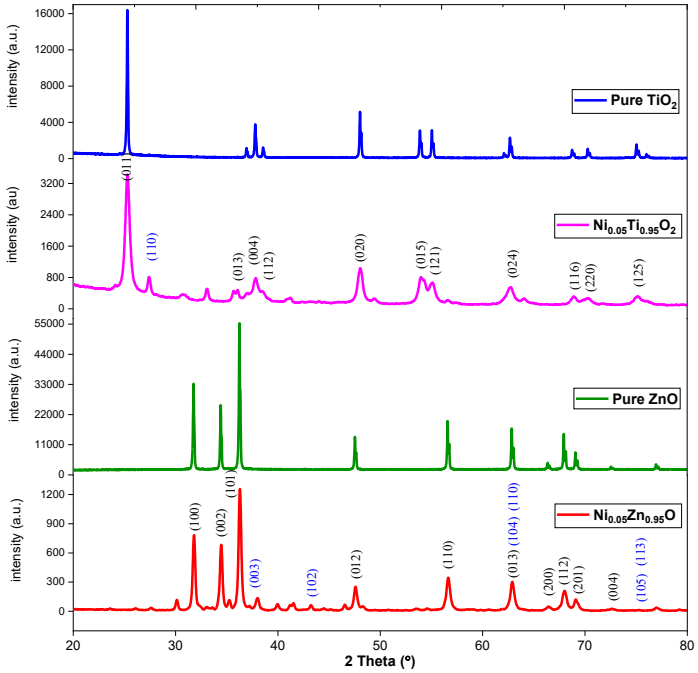

Figure 2. XRD patterns of ZnO, TiO_2, and photocatalyst synthesized by immersion-assisted co-precipitation technique.

c. SEM-EDX characterization

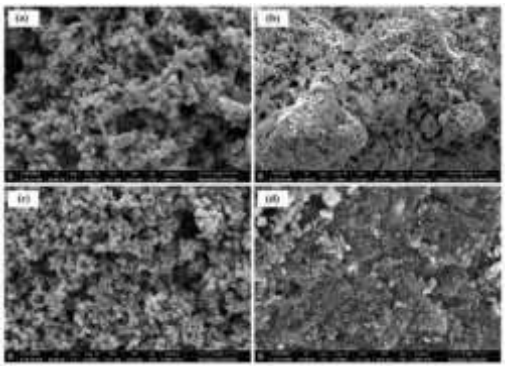

Figure 3. SEM image of (a) Pure ZnO at 10000x magnification; (b) $Ni_{0.05}Zn_{0.95}O$ at 2000x magnification; (c) pure TiO_2 at 10000x magnification; and (d) $Ni_{0.05}Ti_{0.95}O_2$ at 10000x magnification.

Figure 3. shows SEM images of ZnO, TiO_2, and 5% Ni-doped ZnO/TiO_2 respectively. Micrographs show a variety of samples with particle morphology, e.g., round, hexagonal and

Multidisciplinary Indonesian Center Journal (MICJO)
Journal page is available to
https://e-jurnal.jurnalcenter.com/index.php/micjo
Email: admin@jurnalcenter.com

oval. Due to the Ni doping, the particles have smaller sizes with better distribution and tend to form agglomerations than pure TiO_2 and ZnO. As a further indication, accumulation is characterized by a decrease in crystal size and intensity based on the previous XRD analysis. In a study, Fabbiyola *et al*. (Fabbiyola et al., 2017) observed that accumulation is associated with increased attractive forces between particles due to the rise in surface area to volume ratio. In the case of $Ni_{0.05}Ti_{0.95}O_2$, due to the reactive nature of the $Ti[OCH(CH_3)_2]_4$ precursor for water vapor, accumulation can also occur, so it quickly reacts with air to form agglomerates (Fatmawati et al., 2019).

Table 2. Weight and atomic percentage of photocatalyst material based on EDX analysis.

	Pure ZnO		$Ni_{0.05}Zn_{0.95}O$		TiO_2		$Ni_{0.05}Ti_{0.95}O_2$	
Element	Weight (%)	Atomic (%)	Weight (%)	Atomic (%)	Weight (%)	Atomic (%)	Weight (%)	Atomic (%)
O	20.26	37.53	20.29	41.15	48.78	68.58	49.24	72.58
Zn	62.34	28.27	49.01	24.33	-	-	-	-
Ti	-	-	-	-	45.96	21.58	46.41	22.85
Ni	-	-	14.85	8.21	-	-	2.55	1.02
C	8.91	21.99	3.10	8.37	5.26	9.84	1.81	3.54
Na	6.97	8.99	12.48	17.61	-	-	-	-
Al	-	-	0.28	0.33	-	-	-	-
N	1.52	3.22	-	-	-	-	-	-

Table 2 shows weight and atomic percent information based on EDX analysis. It clear that the synthesized material contains several elements other than the targeted Ni as impurities. For example, the element carbon (C) originates in $Ni_{0.05}Ti_{0.95}O_2$ originated from the precursor titanium(IV)isopropoxide $Ti[OCH(CH_3)_2]_4$ and ethanol (C_2H_5OH), the reaction of which forms a carbon chain. In contrast, the elements sodium (Na), aluminium (Al), carbon (C) that were detected in $Ni_{(5\%)}ZnO$ originated from sodium hydroxide (NaOH) solution and aluminium foil impurities when used to cover the sample during preparation. Post-synthetic purification is a step that needs to be maximized to suppress the contaminants in the precipitate. Table 2 shows that, using the immersion-assisted co-precipitation technique, the composition of Ni atoms in the pores of ZnO and TiO_2 were 14.85% and 2.55%, respectively.

Multidisciplinary Indonesian Center Journal (MICJO)
Journal page is available to
https://e-jurnal.jurnalcenter.com/index.php/micjo
Email: admin@jurnalcenter.com

d. Photocatalytic activity on hydrogen gas production.

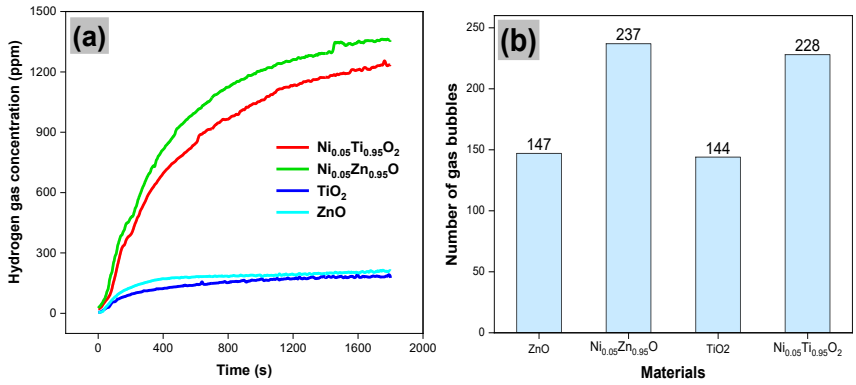

Figure 4. Photocatalytic activity of the material under conditions of 500 rpm with magnetic stirring for yield: (a) concentration of hydrogen gas; (b) air/gas bubbles (H_2+½O_2) observed for 30 minutes.

Figure 4(a) shows the concentration of hydrogen produced in photocatalytic process using MQ-8 gas sensor. The Ni-doped ZnO/TiO_2 photocatalysis clearly shows a significant improvement in hydrogen production over pure ZnO/TiO_2 photocatalyst. Similar trend can be observed in Figure 4(b) that shows the number of hydrogen gas produced expressed in terms of the gas bubbles count. Based on UV-Vis and XRD analysis, the inclusion of Ni dopants into the ZnO and TiO_2 lattices causes a reduction in optical band gap and crystallinity. The decrease in bandgap and crystallinity allows the photocatalyst to increase charge carriers (Seeharaja, P., Kongmuna, P., Paiploda, P., Prakobmit, S., Sriwonga, C., Lohsoontornb, P.K., Vittayakorna, 2019),(Gnanamozhi et al., 2020). On the other hand, the widening of the diffraction peak of the XRD curve suggest a reduction in the size of nanoparticles. Ali *et al*. (Mintu Ali et al., 2021) stated that reducing particle size can minimize charge-transfer barriers and allow easy transition of electrons to the surface, resulting to an increase of photocatalytic efficiency. Here, the average particle size of $Ni_{0.05}Zn_{0.95}O$ (22.47 nm) is smaller than the pure ZnO (65.32 nm), and $Ni_{0.05}Ti_{0.95}O_2$ (21.02 nm) is smaller than TiO_2 (90.46 nm). The decrease in these particles size is inline with the increase in photocatalytic activity when viewed from the correlation of the data in Figure 4 and Table 1. However, the opposite trend is shown by the photocatalyst $Ni_{0.05}Zn_{0.95}O$ (22.47 nm) with $Ni_{0.05}Ti_{0.95}O_2$ (21.02 nm). Although the average particle size of $Ni_{0.05}Zn_{0.95}O$ is larger than $Ni_{0.05}Ti_{0.95}O_2$, the photocatalytic activity of $Ni_{0.05}Zn_{0.95}O$ is higher based on the yield of hydrogen gas concentration and the number of gas bubbles. The photocatalytic reaction was enhanced by a decrease in the overall mean particle size and also by the atomic composition and dopant amounts of Ni. Although both photocatalysts were doped with 5% Ni concentration, EDX analysis in Table 2 shows the weight percentage and atomic composition of Ni in the $Ni_{0.05}Zn_{0.95}O$ photocatalyst are higher than that of $Ni_{0.05}Ti_{0.95}O_2$. This may be responsible for the increase in the yield of hydrogen gas concentration and the more substantial number of bubbles in the case of the $Ni_{0.05}Zn_{0.95}O$ photocatalyst.

Multidisciplinary Indonesian Center Journal (MICJO)
Journal page is available to
https://e-jurnal.jurnalcenter.com/index.php/micjo
Email: admin@jurnalcenter.com

e. Photocatalyst sedimentation

ZnO and TiO_2 photocatalysts are powders whose particles tend to be glutinous or form microscopic agglomerates (Kusmahetiningsih & Sawitri, 2012). Especially in the water medium, the particles quickly accumulate and precipitate. Our observation showed that 1 g of ZnO powder in 100 mL of distilled water was completely precipitated after ±25 minutes. This rapid sedimentation rate poses a challenge in maintaining a stable suspension for effective photocatalytic reactions. To address these physical challenges and keep the particles evenly mixed in the water, we need to look into how well a dispersing agent works. The addition of 0.5 to 1.0 mL of sodium silicate significantly delayed sedimentation for up to ±4 hours. This observation suggests that sodium silicate helps keep the ZnO particles apart by sticking to their surfaces, creating a barrier that prevents them from clumping together. This stabilization is a beneficial alternative to mechanical methods, like constant magnetic stirring, to keep the catalyst from settling at the bottom of the reactor.

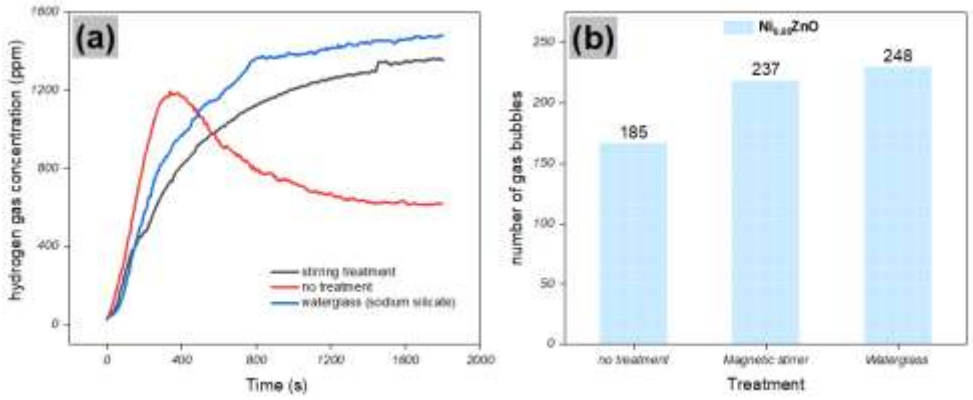

Figure 5. The photocatalytic activity of Ni0.05ZnO with different treatments in generating (a) hydrogen gas concentration; (b) Gas bubbles (H_2+½O_2) count in 30 minutes.

Table 3 Changes in reactor temperature in various observation photocatalytic treatments for Ni0.05ZnO materials

Treatment	Reactor temperature	
	Initial (ºC)	Final (ºC)
no treatment	29	47
magnetic stirrer	30	52
sodium silicate	30	49

Figure 5 shows that the concentration of hydrogen gas generated using a photocatalyst with the help of a magnetic stirrer and water glass is improved. Figure 5(a): Without both treatments, the photocatalyst actually provided a rapid increase in hydrogen gas concentration during the first 400 seconds, but the concentration rapidly declined afterward. Obviously, this decrease can be related to the catalyst sedimentation event, as discussed previously. A study

Multidisciplinary Indonesian Center Journal (MICJO)
Journal page is available to
https://e-jurnal.jurnalcenter.com/index.php/micjo
Email: admin@jurnalcenter.com

explained that adding a certain amount of dispersant can be used to improve the photocatalytic properties because it can reduce the effect of precipitation (Kusmahetiningsih & Sawitri, 2012).

Table 3 shows that the water splitting process is accompanied by a temperature increase in the reactor. In particular, the usage of a magnetic stirrer was observed to give a higher temperature. Some reports suggested that the increase in temperature lowers the efficiency of hydrogen gas harvesting (Huang et al., 2011; Y. Miseki, 2008). According to Huang et al. (Huang et al., 2011), the efficiency decreases because the viscosity of the photocatalytic solution decreases at high temperatures. In addition, the catalyst surface experiences a decrease in the exothermic adsorption capacity of the reactants (Herrmann, 2005). The above phenomenon is connected to how well the water-splitting process works, as the ability of the electron-hole pairs to move to the surface of the photocatalyst particles decreases. Another cause is the electron-hole recombination effect, which also releases energy in the form of heat (Y. Miseki, 2008).

4. CONCLUSION

Ni-doped ZnO and TiO2 photocatalysts were successfully synthesized via immersion-assisted coprecipitation, resulting in a reduction in the band gap energy to 2.87 eV and 2.82 eV, respectively. The addition of 5% Ni significantly reduced the crystallite size to 21 nm, increasing the surface area for hydrogen generation. Most importantly, sodium silicate as a dispersing agent prevented the nanopowder from settling too quickly, making the suspension stable for 4 hours instead of 25 minutes. This chemical stabilization also kept the reactor temperature lower (49°C) than mechanical stirring (52°C), which improved the gas harvesting process. $Ni_{0.05}Zn_{0.95}O_2$ performed best among all samples due to its better Ni atomic composition and better colloidal stability. These results demonstrate that combining Ni doping with chemical dispersion is a highly effective way to split water using photocatalysis.

5. REFERENCES

A. Mills and S. Le Hunte. (1997). An overview of semiconductor photocatalysis. In Journal of Photochemistry and Photobiology A: Chemistry (Vol. 108, pp. 1–35). https://doi.org/https://doi.org/10.1016/S1010-6030(97)00118-4

Anna V. Abramovaa,⁎ , Vladimir O. Abramova, Vadim M Bayazitova, Y. V., & Elena A. Straumalb, Sergey A. Lermontovb, Tatiana A. Cherdyntsevac, Patrick Braeutigamd, Maik Weißed, K. G. (2020). A sol-gel method for applying nanosized antibacterial particles to the surface of textile materials in an ultrasonic field. Ultrasonics - Sonochemistry, 60. https://doi.org/https://doi.org/10.1016/j.ultsonch.2019.104788

Beydoun, D., Amal, R., Low, G., & McEvoy, S. (1999). Role of nanoparticles in photocatalysis. In Journal of Nanoparticle Research (Vol. 1, Issue 4, pp. 439–458). https://doi.org/10.1023/A:1010044830871

Bouaoud, A., Rmili, A., Ouachtari, F., Louardi, A., Chtouki, T., Elidrissi, B., & Erguig, H. (2013). Transparent conducting properties of Ni doped zinc oxide thin films prepared by

Multidisciplinary Indonesian Center Journal (MICJO)
Journal page is available to
https://e-jurnal.jurnalcenter.com/index.php/micjo
Email: admin@jurnalcenter.com

a facile spray pyrolysis technique using perfume atomizer. In Materials Chemistry and Physics (Vol. 137, Issue 3, pp. 843–847). https://doi.org/10.1016/j.matchemphys.2012.10.023

Elilarassi, R., & Chandrasekaran, G. (2011). Synthesis, structural and optical characterization of Ni-doped ZnO nanoparticles. In Journal of Materials Science: Materials in Electronics (Vol. 22, Issue 7, pp. 751–756). https://doi.org/10.1007/s10854-010-0206-8

Engge, Y., Maulana, F., Nurhuda, M., & Istiroyah. (2021). Dissociation of water into hydrogen and oxygen through a combination of electrolysis and photocatalyst. IOP Conference Series: Earth and Environmental Science, 743(1). https://doi.org/10.1088/1755-1315/743/1/012054

Engge, Y., Maulana, F., Nurhuda, M., Istiroyah, I., & Hakim, L. (2023). Enhancing Hydrogen Production through Integration of Electrolysis and Photocatalysis in a Cell. International Journal of Energy Research, 2023, 10. https://doi.org/https://doi.org/10.1155/2023/9881469

Fabbiyola, S., Sailaja, V., Kennedy, L. J., Bououdina, M., & Vijaya, J. J. (2017). Optical and magnetic properties of Ni-doped ZnO nanoparticles. Journal of Alloys and Compounds Journal, 694, 522–531. https://doi.org/10.1016/j.jallcom.2016.10.022

Fatmawati, D., Aritonang, A. B., & Nurlina. (2019). SINTESIS DAN KARAKTERISASI TiO2-KAOLIN MENGGUNAKAN METODE SOL GEL. In Jurnal Kimia Khatulistiwa (Vol. 8, Issue 2, pp. 15–21). https://jurnal.untan.ac.id/index.php/jkkmipa/article/view/36559

Ganesh, I., Gupta, A. ., Sekhar, P. S. ., Radha, K., Padmanabham, G., & Sundararajan, G. (2012). Preparation and Characterization ofNi-Doped TiO2 Materials for Photocurrent and Photocatalytic Applications. The Scientific World Journal. https://doi.org/10.1100/2012/127326

Gnanamozhi, P., Renganathan, V., Chen, S. M., Pandiyan, V., Antony Arockiaraj, M., Alharbi, N. S., Kadaikunnan, S., Khaled, J. M., & Alanzi, K. F. (2020). Influence of Nickel concentration on the photocatalytic dye degradation (methylene blue and reactive red 120) and antibacterial activity of ZnO nanoparticles. In Ceramics International (Vol. 46, Issue 11, pp. 18322–18330). https://doi.org/10.1016/j.ceramint.2020.05.054

Gupta, S. M., & Tripathi, M. (2011). A review of TiO2 nanoparticles. Chinese Science Bulletin, 56(16), 1639–1657. https://doi.org/10.1007/s11434-011-4476-1

Herrmann, J. M. (2005). Heterogeneous photocatalysis: State of the art and present applications. Topics in Catalysis, 34(1–4), 49–65. https://doi.org/10.1007/s11244-005-3788-2

Huang, C., Yao, W., T-Raissi, A., & Muradov, N. (2011). Development of efficient photoreactors for solar hydrogen production. Solar Energy, 85(1), 19–27. https://doi.org/10.1016/j.solener.2010.11.004

Istiroyah, Engge, Y., Maulana, F., & Nurhuda, M. (2021). Literature review of the development of ZnO and TiO2as photocatalytic material in water splitting processes. IOP Conference

Multidisciplinary Indonesian Center Journal (MICJO)
Journal page is available to
https://e-jurnal.jurnalcenter.com/index.php/micjo
Email: admin@jurnalcenter.com

Series: Earth and Environmental Science, 743(1). https://doi.org/10.1088/1755-1315/743/1/012068

Kusmahetiningsih, N., & Sawitri, D. (2012). Aplikasi TiO2 Sebagai Self Cleaning pada Cat Tembok dengan Dispersant Polietilen Glikol (PEG). JURNAL TEKNIK POMITS, 1(1), 1–5.

Lin, Y.-J., Chang, Y.-H., Yang, W.-D., & Tsai, B.-S. (2006). Synthesis and characterization of ilmenite NiTiO3 and CoTiO3 prepared by a modified Pechini method. Journal of Non-Crystalline Solids, 352, 789–794. https://doi.org/10.1016/j.jnoncrysol.2006.02.001

Luévano-Hipólito, E., & Torres-Martínez, L. . (2017). Sonochemical synthesis of ZnO nanoparticles and its use as photocatalyst in H2 generation. Materials Science & Engineering B, 226, 223–233. https://doi.org/10.1016/j.mseb.2017.09.023 Received

Mallikarjunaswamy, C Lakshmi Ranganatha, V Ramu, R., Udayabhanu, & Nagaraju, G. (2019). Facile microwave-assisted green synthesis of ZnO nanoparticles: application to photodegradation, antibacterial and antioxidant. Journal of Materials Science: Materials in Electronics. https://doi.org/10.1007/s10854-019-02612-2

Maulana, F., Engge, Y., Nurhuda, M., & Istiroyah. (2022). Effect of Voltage Source Differences on Hydrogen Gas Production by Electrolysis-photocatalysis Reactor Systems. IOP Conf. Series: Earth and Environmental Science. https://doi.org/10.1088/1755-1315/1097/1/012049

Maulana, F., Engge, Y., Nurhuda, M., Istiroyah, I., Juwono, A. M., & Hakim, L. (2024). Boosting Hydrogen Production through Water Splitting : N , Ni , and N-Ni Doped ZnO Photocatalysts. Journal of The Electrochemical Society, 171(4), 46505. https://doi.org/10.1149/1945-7111/ad3d0f

Mintu Ali, M., Jahidul Haque, M., Humayan Kabir, M., Abdul Kaiyum, M., & Rahman, M. . (2021). Nano synthesis of ZnO–TiO2 composites by sol-gel method and evaluation of their antibacterial, optical and photocatalytic activities. Results in Materials Journal, 11. https://doi.org/10.1016/j.rinma.2021.100199

Murakami, N., Chiyoya, T., Tsubota, T., & Ohno, T. (2008). Switching redox site of photocatalytic reaction on titanium(IV) oxide particles modified with transition-metal ion controlled by irradiation wavelength. In Applied Catalysis A: General (Vol. 348, Issue 1, pp. 148–152). https://doi.org/10.1016/j.apcata.2008.06.040

Pavithra, M., & Jessie Raj, M. . (2021). Influence of ultrasonication time on solar light irradiated photocatalytic dye degradability and antibacterial activity of Pb doped ZnO nanocomposites. Ceramics International. https://doi.org/10.1016/j.ceramint.2021.08.128

Samanta, A., Goswami, M. N., & Mahapatra, P. K. (2018). Magnetic and electric properties of Ni-doped ZnO nanoparticles exhibit diluted magnetic semiconductor in nature. In Journal of Alloys and Compounds (Vol. 730, pp. 399–407). https://doi.org/10.1016/j.jallcom.2017.09.334

Seeharaja, P., Kongmuna, P., Paiploda, P., Prakobmit, S., Sriwonga, C., Lohsoontornb, P.K., Vittayakorna, N. (2019). Ultrasonically-assisted surface modified TiO2/rGO/CeO2

Multidisciplinary Indonesian Center Journal (MICJO)
Journal page is available to
https://e-jurnal.jurnalcenter.com/index.php/micjo
Email: admin@jurnalcenter.com

heterojunction photocatalysts for conversion of CO2 to methanol and ethanol (Vol. 58, Issue June). Elsevier. https://doi.org/https://doi.org/10.1016/j.ultsonch.2019.104657

Selvinsimpson, S., Gnanamozhi, P., Pandiyan, V., Govindasamy, M., Habila, M. A., Almasoud, N., & Chen, Y. (2021). Synergetic effect of Sn doped ZnO nanoparticles synthesized via ultrasonication technique and its photocatalytic and antibacterial activity. Environmental Research Journal. https://doi.org/10.1016/j.envres.2021.111115

Shahi, K., Singh, R. S., Singh, J., Aleksandrova, M., & Singh, A. K. (2020). Synthesis of Ag Nanoparticle-Decorated ZnO Nanorods Adopting the Low-Temperature Hydrothermal Method. In Journal of Electronic Materials (Vol. 49, Issue 1, pp. 637–642). https://doi.org/10.1007/s11664-019-07771-w

Singh, B., Kaushal, A., Bdikin, I., Venkata Saravanan, K., & Ferreira, J. M. F. (2015). Effect of Ni doping on structural and optical properties of Zn1-xNixO nanopowder synthesized via low cost sono-chemical method. In Materials Research Bulletin (Vol. 70, pp. 430–435). https://doi.org/10.1016/j.materresbull.2015.05.009

Y. Miseki, . A. Kudo. (2008). Heterogeneous photocatalyst materials for water splitting. Chemical Society Reviews, 253–278. https://doi.org/10.1039/b800489g